

COMPARISON OF INTERCONTINENTAL AEROSOLS: DESERT AND MONSOON-INFLUENCED REGIONS

AIM:

This research project was undertaken to compare the optical and physical properties of aerosols at the 0.440 μ m, 0.675 μ m, 0.870 μ m and 1.020 μ m spectral wavelengths between desert and monsoon-influenced regions. In this project, Zinder, one of the popular cities in the Republic of Niger and Beijing, the capital city of China were chosen to represent desert and monsoon influenced regions respectively.

Place and Duration of Study:

Four years of Aerosol Optical Depth (AOD) data were extracted from level 2.0 quality-assured almucantar version products of AERONET data, at both Beijing-CAM (39.933°N, 116.317°E) and Zinder Airport (13.775°N, 8.984°E) between 2012 and 2015.

Methodology:

In this research project, physical and optical properties of aerosols were determined using Angstrom equations. Angstrom exponent, curvature, turbidity coefficient and spectral variation of the aerosols in Zinder Airport and Beijing-CAM were calculated and the results were then compared. Both the physical and optical properties of the aerosols were determined from the calculated values.

Results:

The results obtained indicated that there were dominant coarse-mode aerosol particles in Zinder city, while fine-mode aerosol particles were found in Beijing. The results also showed that the overall Aerosol Optical Depth (AOD) in Zinder is higher than that of Beijing, but the atmosphere of Beijing was hazier than that of Zinder.

Conclusion:

The prevalence of coarse-mode particle sizes in Zinder was due to desert dust particles in the region, while the prevalence of fine-mode particles in Beijing was due to anthropogenic aerosol particle generation in the region, which may result from heavy industrialization in China. The higher aerosol loading in Zinder is responsible for absorbing light coming from the sun which, in turn, makes the atmosphere clear, while the lower aerosol loading in Beijing is responsible for scattering light coming from the sun, thereby obstructing the atmospheric visibility in the region.

Keywords: Angstrom exponent, Turbidity coefficient, Aerosol Optical Depth, Curvature, AERONET

1.0 Introduction

Apart from green-house gases, aerosols are another important agent of radiative forcing that affects the planet Earth [1-3]. Aerosols affect our environment [1-3], influences cloud formation [4], and cause overall increases or decreases in atmospheric temperature [5]. Aerosols also affect human health by penetrating deep into respiratory system and ultimately the cardiovascular system [6, 7]. These effects of aerosols make it necessary to monitor them via

both ground-based observation and satellite [4, 8, and 9]. However, it is difficult to monitor aerosol properties via satellite, because satellites always rely on backscattering signals, which are more often than not contaminated signals [10]. This is the reason why ground-based measurements are more commonly used to get accurate aerosol data since the ground-based instruments are mounted to take measurements directly facing the sun.

There are a number of ground-based Sun-photometer networks across the globe that are used for aerosol monitoring. These include SKY-Radiometer network (SKYNET) and Aerosol Robotic Network (AERONET). AERONET is a very popular and reliable source of aerosol data. It provides measurements from over 400 data stations worldwide for accurate retrieval of aerosol optical depth (AOD), single scattering albedo (SSA) and aerosol particle size distribution (PSD) by taking into account direct solar measurement and scattering measurement [14,15]. AERONET became a yardstick for satellite AOD retrieval [16, 17]. Two of the AERONET data stations are Beijing-CAM in China and Zinder Airport in the Republic of Niger.

Beijing is the capital city of China and it is located in North-China, the East-Asian region, situated at longitude 116.317⁰E and latitude 39.9330N, with a population of more than 19 million [18]. Beijing is located at the warm temperate zone, half moist continental monsoon climate, featuring four distinct seasons: Arid multi-windy spring; hot and multi-rain summer; sunny and fresh autumn, and cold and dry winter. Beijing has experienced rapid economic development over the several decades. Beijing shows distinct seasonal transitions. Atmospheric pollution is a problem in Beijing because it affects human activities and is triggered by frequent dust storm events in the city. Zinder, on the other hand, is one of the most popular cities in the Niger Republic. It is located at Longitude 8.984⁰ E and Latitude 13.775⁰ N in the West-African sub-region. It is typically characterized as a Sahara desert area with virtually no rainfall. The arid nature of Zinder makes it possible for dust to prevail and cause haze in the atmosphere. Figures 1a and 1b respectively depict Beijing and Zinder.

This study was designed to find correlation between aerosol particle size distribution (PSD), aerosol optical depth (AOD) and atmospheric visibility in the two cities, using four years worth of level 2.0 AERONET data collected in Beijing-CAM and Zinder airport from 2012 to 2015.



Figure 1a: Map of Niger with its main cities



Figure 1b: Map of China with some main cities

2.0 Materials and Method

Four years (2012-2015) of level 2.0, 'quality-assured' AOD data from Zinder and Beijing were extracted from the AERONET database using the standard retrieval procedure for AERONET products. These raw data archive files were unpacked using the WinRAR 4.11 wizard, and viewed using Microsoft Excel. The AOD data used were measured at four spectral bands, namely: 440 nm, 675 nm, 870 nm and 1020 nm.

Annual median averages of the AODs with their corresponding wavelengths were computed and arranged in tabular forms. Statistical comparison between annual AOD in Zinder and that of Beijing was performed.

The annual mean AODs of Zinder and Beijing were plotted against their corresponding wavelengths and the equations for graphs were fitted using second order polynomial curves with natural logarithmic

coordinates, using least square fitting algorithm to calculate the Angstrom coefficients for both Zinder and Beijing. The Angstrom coefficients that were calculated were Curvature (α_2) and Turbidity (β).

The AOD equation is given as:

$$\tau = \beta \lambda^{-\alpha} \quad (1)$$

The linear equation that links the natural-logarithmic AOD and the corresponding natural-logarithmic wavelength is:

$$\ln \tau = -\alpha \ln \lambda + \beta \quad (2)$$

The second order polynomial equation relating the AOD and the wavelength in natural logarithmic form is:

$$\ln \tau = \alpha_2 \ln^2 \lambda + \alpha_1 \ln \lambda + \beta \quad (3)$$

Where: τ is the AOD; α_2 is the curvature; β is the turbidity coefficient; α is the Angstrom exponent.

Angstrom equation was also used to calculate the annual Angstrom exponents in each city. The expression for Angstrom exponent is given as:

$$\alpha = - \frac{d \ln \tau}{d \ln \lambda} \quad (4)$$

Spectral variation of AOD (α') was also determined using the second derivative of Angstrom exponent (α)

$$\alpha' = \frac{d\alpha}{d \ln \lambda} = -2\alpha_2 \quad (5)$$

The values of α_2 , β , R^2 and α' were presented in a tabular form. Where: R^2 is the least square value of the residual.

3.0 Results and Discussions

Variation of annual median AODs in both Zinder and Beijing at four different spectral wavelengths, from the year 2012 to the year 2015 are presented in Figure 2 below. The AODs in each case decreased with a corresponding increase in wavelength. This decreasing trend of AOD with wavelength was presented in Figures 2a-2d.

Table 1 represents difference between AOD in Zinder and Beijing. In each year, the average AOD value of Beijing was subtracted from that of Zinder and the results were tabulated. The negative values obtained in 2013 and 2014 at 0.440 μm indicated that the AODs in Beijing at that wavelength are higher than that in Zinder.

Values of $\beta < 0.1$ signify relatively clear atmospheres, while values of $\beta > 0.2$ signify relatively hazy atmosphere [23]. Based on this convention, since values of β from Table 2 were all greater than

0.2, then the conclusion is that the overall atmospheric status in both Zinder and Beijing was hazy from 2012 to 2015. In Table 2, Beijing displayed maximum haze status in 2012 with a β -value 0.72 and minimum haze status in 2014 with a β -value 0.416. On the other hand, Zinder displayed maximum haze status of β -value 0.640 in 2012 and minimum haze status of β -value 0.300 in 2014.

Table 1: Annual Difference between AOD in Zinder and Beijing at Four Spectral Wavelengths.

Wavelength	Difference between AOD in Zinder and Beijing			
λ (μm)	2012	2013	2014	2015
0.440	0.028	-0.013	-0.046	0.149
0.675	0.093	0.110	0.011	0.232
0.870	0.108	0.128	0.017	0.243
1.020	0.126	0.134	0.022	0.241

Table 2: Angstrom Parameters in Zinder and Beijing, 2012-2015

Year	α_2		β		R^2		α		α'	
	Zinder	Beijing	Zinder	Beijing	Zinder	Beijing	Zinder	Beijing	Zinder	Beijing
2012	0.329	0.570	0.640	0.792	0.999	0.996	0.580	1.256	-0.658	-1.140
2013	0.154	0.844	0.561	0.988	1.000	0.995	0.354	1.135	-0.308	-1.688
2014	0.172	0.506	0.382	0.632	1.000	0.995	0.710	1.170	-0.344	-1.012
2015	-	0.540	0.502	0.663	0.998	0.996	0.222	1.115	-	-1.080

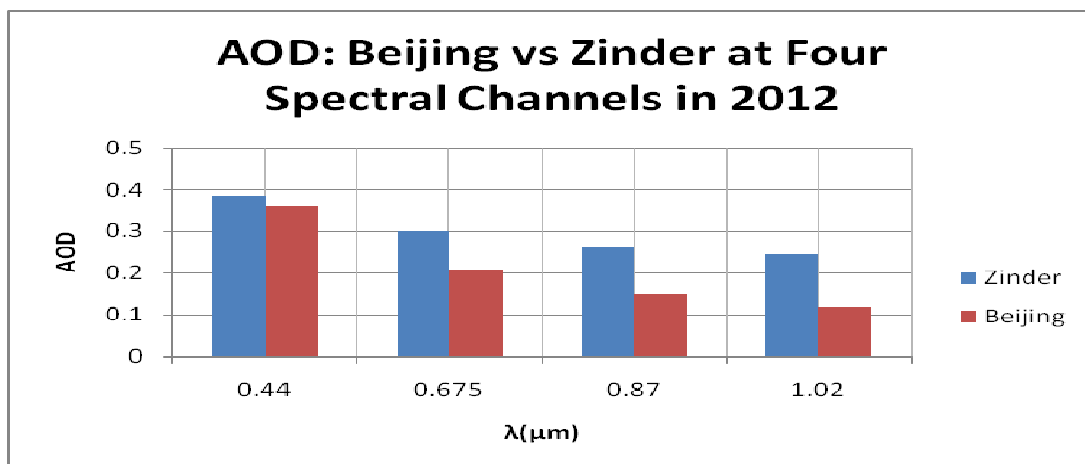
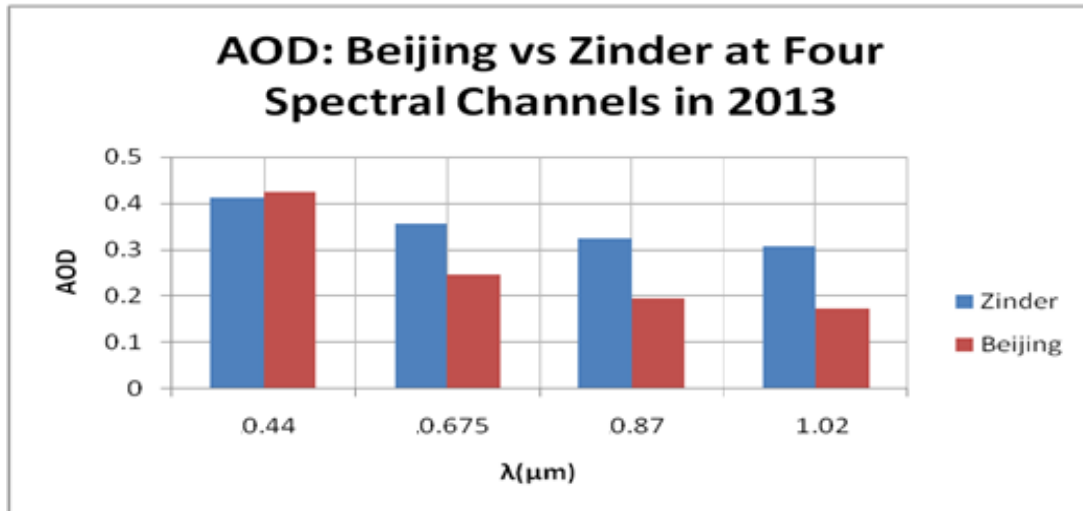
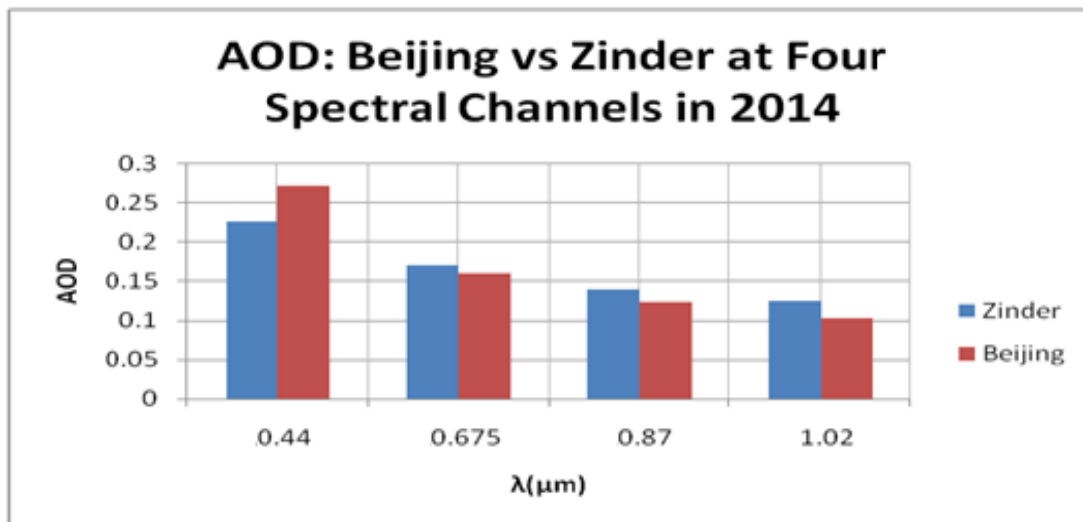


Figure 2a



102

103 Figure 2b



104

105 Figure 2c

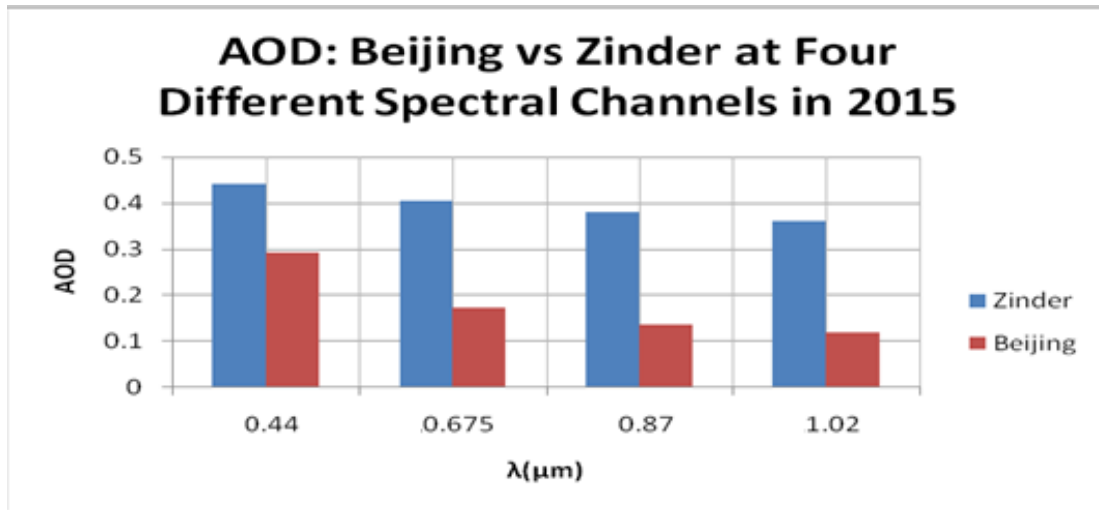


Figure 2d

Figure 2: Comparison of Annual AOD between Zinder and Beijing Cities

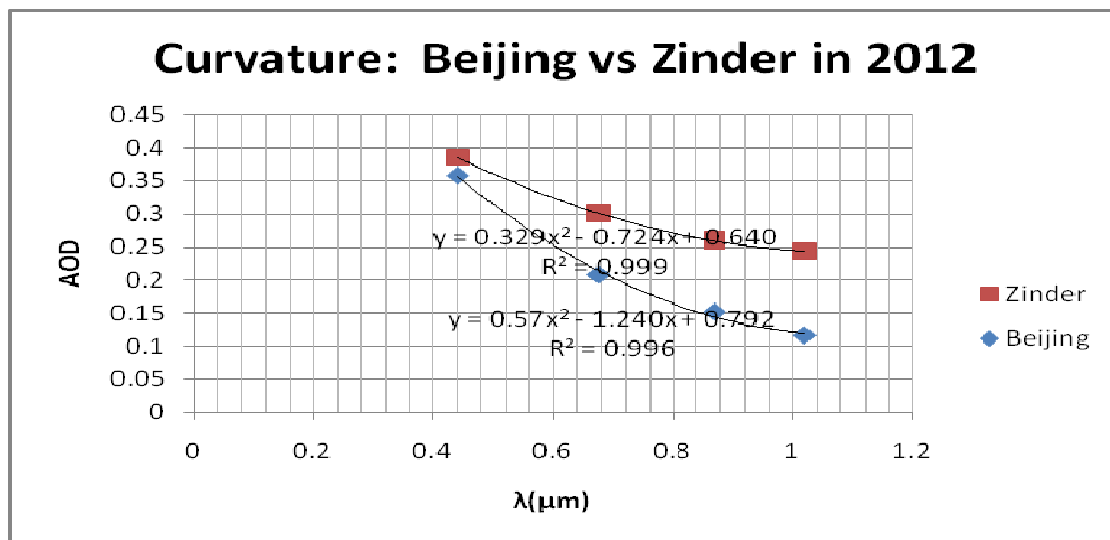


Figure 3a

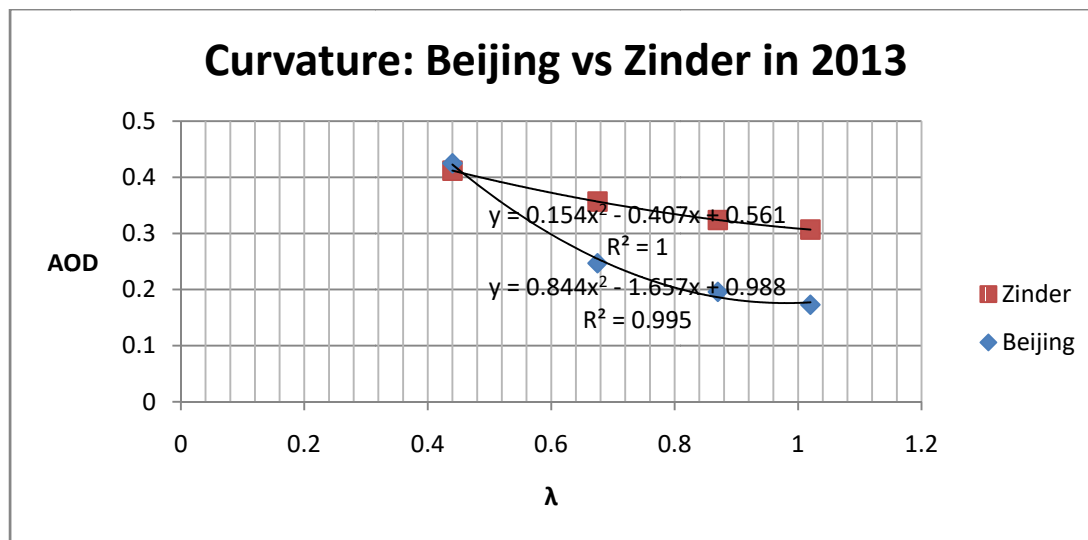


Figure 3b

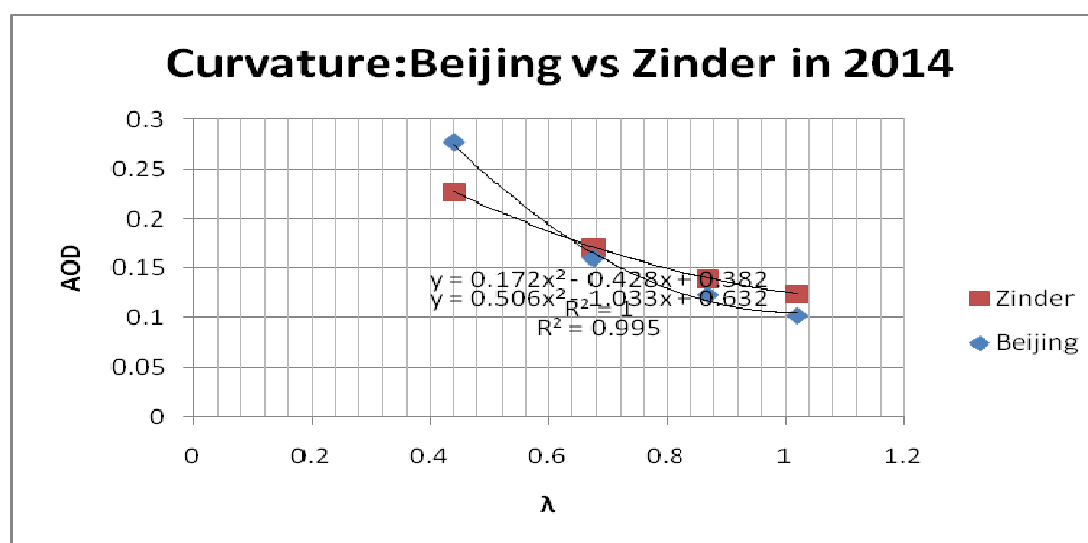


Figure 3c

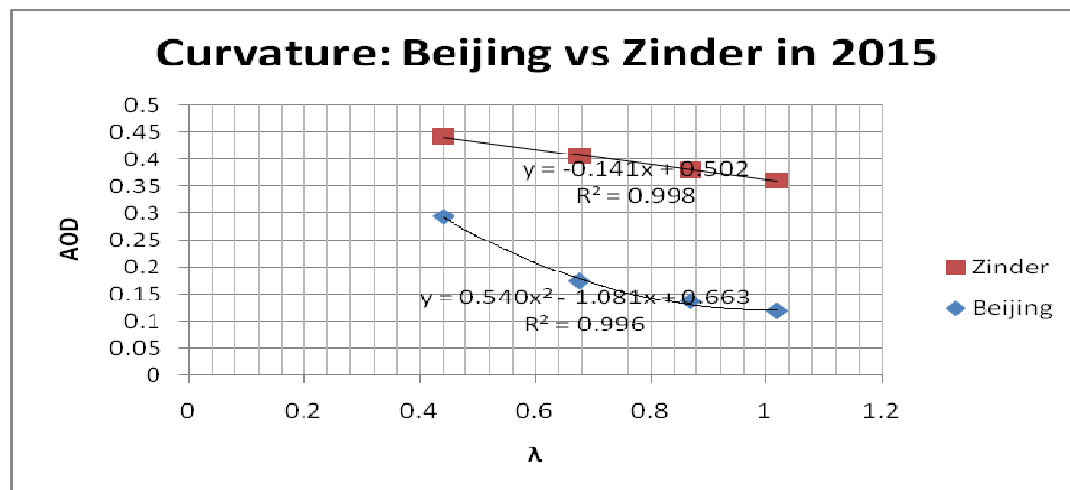


Figure 3d

Figure 3: Comparison of Curvature and Turbidity Coefficient between Zinder and Beijing Cities.

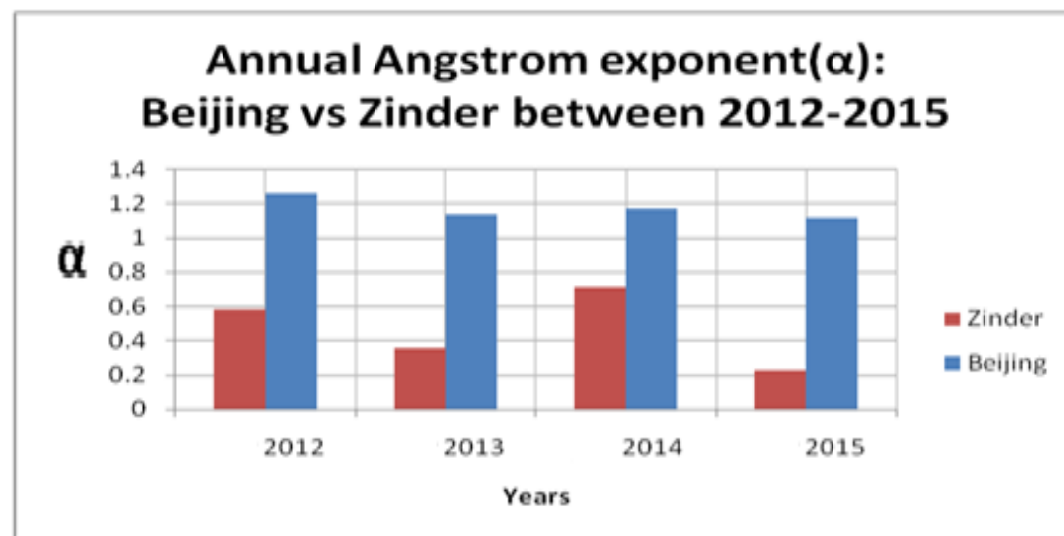


Figure 4: Comparison of Angstrom Exponent between Zinder and Beijing.

AOD changes with spectral wavelength and this is called the curvature. Studies show that curvature of coarse mode aerosol particles and that of bimodal aerosol particles in which coarse mode is dominant always appear positive. It changes rapidly with aerosol properties and it affects the value of α' . From Table 2, all α_2 -values were positive, which indicates prevalence of coarse mode particles in both Beijing and Zinder.

However, the curvature of $\ln \tau$ versus $\ln \lambda$ was found to be negative for biomass burning aerosols in Bolivia and Zambia, and for urban industrial aerosol in USA [22]. Based on this report, it is possible that fine-mode particles that were claimed to be more than 50% of the aerosol are not

that high in Beijing. That is why the curvature did not appear to be concave as typically found with fine-mode particles. In Beijing, dust storms are very common and it is possible that the dust events dominate fine particles from anthropogenic sources. Throughout the four years, Beijing displayed higher values of α_2 than Zinder, which can be seen from Table 2. The curvature is also obvious on the curves in Figures 3a-3d. Nevertheless, in 2015, a linear fit was found to be the best fit for AOD data in Zinder. This is because, the curvature in that case was found to be very small which was considered insignificant and this necessitated the use of linear fit, instead of the second-order polynomial fit. In this case the conclusion was that the small value of the curvature was due to bimodal aerosol size distribution dominated by coarse mode particles [22].

From Figure 3, it is obvious that the AODs are changing with wavelengths faster in Beijing than in Zinder. These changes are represented by the curvature on the graphs in Figure 3. The curvature occurs due to change in aerosol type [22]. Curvature is more pronounced under high turbidity condition, because anthropogenic aerosols are responsible for light scattering and are made up of different types of aerosols. This implies that low curvature is associated with high AOD and high α -values and vice versa. In Beijing, there is more than one aerosol type and this is expected in a mega-city like Beijing with a population of more than 19 million. Fine-mode aerosol particles are expected from human activities in the city and coarse-mode aerosols particles are expected from dust storms which are very frequent in Beijing.

With regard to particle size characterization in each city, although aerosol particles size can be determined using volume concentration in 22 radius bins, the angstrom exponent values were used instead as an index for the characterization. Conventionally, values of α range are between zero and two (0-2); fine-modes of aerosol particles take values of >0.6 , while coarse-modes take lesser values of <0.6 . [11, 19 and 20]. From Table 2, all α -values in Beijing were >0.6 . This indicates the prevalence of fine mode particles in Beijing. In Beijing, the fine mode fraction was greater than 50% and was more than 70% in summer [21]. Average α -values in Beijing recorded in the year 2016 were from around 1.0 in 2005 to around 1.1 in 2014 [21]. This α -value of 1.1 in 2014 agrees very well with our value of 1.170 recorded in 2014. For Zinder, on the other hand, α -values were <0.6 . This indicates dominance of coarse mode particles in the region. However, the α -value recorded in 2014 was 0.710 which indicates dominance of fine mode particles according to [22]. This might be due to instrumentation error, meteorological factors or inadequacy of the Angstrom formula used in the calculation. However, it was reported that any value of α on the order of zero can be considered as coarse-mode [22]. Based on this report, the α -value of 0.710 is an indicator of coarse mode, mixed with reasonable amounts of fine-mode particles. The domination of coarse mode particles in Zinder was due to the fact that Zinder is in a Sahara region which is typically characterized with dust aerosol. Comparison of the Angstrom exponent between Zinder and Beijing was given in Figure 4.

4.0 Conclusion

Based on observation and retrieval of aerosol data from two AERONET sites in Zinder and Beijing, from 2012 to 2015, aerosol optical depth (AOD), Angstrom exponent (α), turbidity coefficient as well as curvature of each city were analyzed and compared to assess the variability and similarity of physical and optical properties of aerosol in the two cities. The results indicate that the coarse-mode particles dominate in Zinder due to desert dust prevalence the four years of the study. On the other hand, show that there is a mixture of fine-mode and coarse-mode particles in Beijing. The result also revealed that both Zinder and Beijing atmospheres were typically characterized with haze due to dust (in the case of Zinder) and due to dust storm and excessive anthropogenic aerosol release in the atmosphere (in the case of Beijing). In case of Zinder, the desert dust absorbs more light than it scatters, thereby causing less haze. In Beijing, the anthropogenic aerosols, which are dominant, scatter more light than it absorbs, thereby causing more haze in the region.

5.0 References

- [1] Zhou, M.G.; Liu, Y.N.; Wang, L.J.; Kuang, X.Y.; Xu, X.H.; Kan, H.D. Particulate air pollution and mortality in a cohort of chinese men. *Environ. Pollut.* 2014, 186, 1–6.
- [2] Langrish, J.P.; Mills, N.L. Air pollution and mortality in europe. *Lancet* 2014, 383, 758–760.
- [3] Schwartz, J.; Neas, L.M. Fine particles are more strongly associated than coarse particles with acute respiratory health effects in schoolchildren. *Epidemiology* 2000, 11, 6–10.
- [4] Sayer, A.M.; Munchak, L.A.; Hsu, N.C.; Levy, R.C.; Bettenhausen, C.; Jeong, M.J. MODIS collection 6 aerosol products: Comparison between aqua's e-deep blue, dark target, and "merged" data sets, and usage recommendations. *J. Geophys. Res. Atmos.* 2014, 119, 13965–13989.
- [5] Li, Z.Q.; Niu, F.; Fan, J.W.; Liu, Y.G.; Rosenfeld, D.; Ding, Y.N. Long-term impacts of aerosols on the vertical development of clouds and precipitation. *Nat. Geosci.* 2011, 4, 888–894.
- [6] Janssen, N.A.H.; Fischer, P.; Marra, M.; Ameling, C.; Cassee, F.R. Short-term effects of PM_{2.5}, PM₁₀ and PM_{2.5-10} on daily mortality in the Netherlands. *Sci. Total Environ.* 2013, 463, 20–26.
- [7] Bergen, S.; Sheppard, L.; Sampson, P.D.; Kim, S.Y.; Richards, M.; Vedal, S.; Kaufman, J.D.; Szpiro, A.A. A national prediction model for PM_{2.5} component exposures and measurement error-corrected health effect inference. *Environ. Health Perspect.* 2013, 121, 1017–1025.
- [8] Levy, R.C.; Mattoo, S.; Munchak, L.A.; Remer, L.A.; Sayer, A.M.; Patadia, F.; Hsu, N.C. The collection 6 MODIS aerosol products over land and ocean. *Atmos. Meas. Tech.* 2013, 6, 2989–3034.

217 [9] Remer, L.A.; Kaufman, Y.J.; Tanre, D.; Mattoo, S.; Chu, D.A.; Martins, J.V.; Li, R.R.; Ichoku,
218 C.; Levy, R.C.; Kleidman, R.G.; et al. The MODIS aerosol algorithm, products, and validation. *J.*
219 *Atmos. Sci.* 2005, 62, 947–973.

220 [10] Tao, M.H.; Chen, L.F.; Wang, Z.F.; Tao, J.H.; Che, H.Z.; Wang, X.H.; Wang, Y. Comparison
221 and evaluation of the MODIS collection 6 aerosol data in China. *J. Geophys. Res. Atmos.* 2015,
222 120, 6992–7005.

223 [11] Dubovik, O.; Smirnov, A.; Holben, B.N.; King, M.D.; Kaufman, Y.J.; Eck, T.F.; Slutsker, I.
224 Accuracy assessments of aerosol optical properties retrieved from aerosol robotic network
225 (AERONET) sun and sky radiance measurements. *J. Geophys. Res. Atmos.* 2000, 105, 9791–
226 9806.

227 [12] Che, H.; Shi, G.; Uchiyama, A.; Yamazaki, A.; Chen, H.; Goloub, P.; Zhang, X.
228 Intercomparison between aerosol optical properties by a prede skyradiometer and cimel
229 sunphotometer over Beijing, China. *Atmos. Chem. Phys.* 2008, 8, 3199–3214.

230 [13] Eck, T.F.; Holben, B.N.; Dubovik, O.; Smirnov, A.; Goloub, P.; Chen, H.B.; Chatenet, B.;
231 Gomes, L.; Zhang, X.Y.; Tsay, S.C.; et al. Columnar aerosol optical properties at aeronet sites
232 in central Eastern Asia and aerosol transport to the tropical Mid-Pacific. *J. Geophys. Res.*
233 *Atmos.* 2005, 110.

234 [14] Schuster, G.L.; Vaughan, M.; MacDonnell, D.; Su, W.; Winker, D.; Dubovik, O.; Lapyonok,
235 T.; Trepte, C. Comparison of calipso aerosol optical depth retrievals to aeronet measurements,
236 and a climatology for the lidar ratio of dust. *Atmos. Chem. Phys.* 2012, 12, 7431–7452.

237 [15] Garcia, O.E.; Diaz, J.P.; Exposito, F.J.; Diaz, A.M.; Dubovik, O.; Derimian, Y.; Dubuisson,
238 P.; Roger, J.C. Shortwave radiative forcing and efficiency of key aerosol types using aeronet
239 data. *Atmos. Chem. Phys.* 2012, [12] 5129–5145.

240 [16] Lee, J.; Kim, J.; Yang, P.; Hsu, N.C. Improvement of aerosol optical depth retrieval from
241 MODIS spectral reflectance over the global ocean using new aerosol models archived from
242 aeronet inversion data and tri-axial ellipsoidal dust database. *Atmos. Chem. Phys.* 2012, 12,
243 7087–7102.

244 [17] Mi, W.; Li, Z.; Xia, X.; Holben, B.; Levy, R.; Zhao, F.; Chen, H.; Cribb, M. Evaluation of the
245 moderate resolution imaging spectroradiometer aerosol products at two aerosol robotic network
246 stations in China. *J. Geophys. Res. Atmos.* 2007, 112.

247 [18] Zhang, A.; Qi, Q.; Jiang, L.; Zhou, F.; Wang, J. Population exposure to PM_{2.5} in the urban
248 area of Beijing. *PLoS ONE* 2013, 8, e63486.

249 [19] Xie, Y.; Li, Z.; Li, D.; Xu, H.; Li, K. Aerosol optical and microphysical properties of four
250 typical sites of sonnet in China based on remote sensing measurements. *Remote Sens.* 2015,
251 7, 9928–9953.

- 252 [20] Dubovik, O.; Holben, B.; Eck, T.F.; Smirnov, A.; Kaufman, Y.J.; King, M.D.; Tanre, D.;
253 Slutsker, I. Variability of absorption and optical properties of key aerosol types observed in
254 worldwide locations. *J. Atmos. Sci.* 2002, 59, 590–608.
- 255 [21] Wei Chen , Hongzhao Tang, Haimeng Zhao 3 and Lei Yan , Analysis of Aerosol Properties
256 in Beijing Based on Ground-Based Sun Photometer and Air Quality Monitoring Obs Remote
257 Sens. 2016, 8, 110; doi:10.3390/rs8020110 observations from 2005 to 2014.
- 258 [22] D. G. Kaskaoutis and H. D. Kambezidis, Investigation into the wavelength dependence of
259 the aerosol optical depth in the Athens area, *Q. J. R. Meteorol. Soc.* (2006), 132, pp. 2217–
260 2234.
- 261 [23]D.O. Akpootu and M. Momoh, The Ångström Exponent and Turbidity of Soot Component in
262 the Radiative Forcing of Urban Aerosols, *Nigerian Journal of Basic and Applied Science* (March,
263 2013), 21(1): 70-78.
- 264
- 265